THE JOURNAL OF
PHYSICAL CHEMISTRY
LETTERS
A JOURNAL OF THE AMERICAN CHEMICAL SOCIETY

pubs.acs.org/JPCL Letter

Device-Based Probe of Triplet Exciton Diffusion in Singlet Fission Materials

Tao Zhang, Deepesh Rai, and Russell J. Holmes*

Cite This: *J. Phys. Chem. Lett.* 2021, 12, 966−972 Read Online

ACCESS | Metrics & More | Article Recommendations | SI Supporting Information

ABSTRACT: Probing triplet transport in singlet fission materials can be challenging due to the presence of multiple diffusing species. We present a device-based method to measure the intrinsic triplet diffusion length (L_D) in organic semiconductor thin films exhibiting singlet fission. Triplet states are optically injected into the singlet fission material of interest via energy transfer from an adjacent thin film characterized by strong spin−orbit coupling. Injected triplets migrate through the full thickness of the material before undergoing dissociation at a donor−acceptor interface. By modeling the ratio of injector and acceptor photocurrent as a function of layer thickness, the triplet L_D is extracted separate from processes of unknown efficiency including singlet fission and diffusion. In considering three archetypical fission systems, a wide range is found for the triplet L_D, ranging from 3.3 ± 0.4 nm for 5,12-bis((triisopropylsilyl)ethynyl)tetracene to 17.1 ± 1.3 nm for pentacene and 32.1 ± 2.6 nm for tetracene.

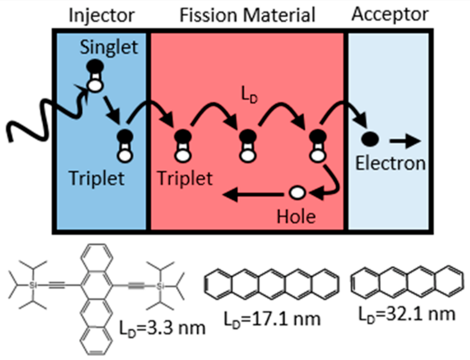

Singlet fission is a photophysical process observed in organic semiconductors that converts a spin zero singlet exciton into two spin unity triplet excitons.[1−6] The energetic requirement to observe singlet fission is that the triplet energy must be roughly half of the associated singlet energy ($E(S_1) \approx 2E(T_1)$). Materials exhibiting singlet fission have received particular interest for applications in photoconversion. Used on their own, singlet fission absorbers are capable of generating two electrons from a single absorbed photon. When combined with conventional silicon-based photovoltaic cells, singlet fission materials offer a route to improve spectral coverage by direct charge generation or reduced thermalization loss via downconversion.[7−10] The latter may involve coupling the singlet fission material to an infrared-emitting species, permitting the conversion of absorbed visible light into infrared radiation that can be efficiently absorbed by silicon. In such instances, the kinetics involved in moving from the singlet to the triplet to the emitter must be optimized for high efficiency. While the kinetics of singlet fission have been studied extensively, specific studies of triplet migration in these materials are more challenging, as it is difficult to isolate triplet transport from the initial fission event and the migration of any remaining singlets.

Singlet fission is a multistep process. A photogenerated singlet on one molecule interacts with a ground state neighboring molecule to form a correlated triplet pair.[11−13] The triplet pair separates into two individual mobile triplet excitons.[1,2] Direct probing of triplet exciton diffusion cannot be performed by using conventional photoluminescence-based measurements since the generated triplets are not typically luminescent.[14] As a result, prior work has utilized singlet exciton fluorescence as an indirect probe of triplet exciton diffusion in the limit of large triplet populations capable of singlet formation via triplet−triplet fusion.[14−16] Similarly, ultrafast transient absorption spectroscopy[17−19] is capable of probing the intrinsic diffusion length of both nonradiative triplets and singlet fission; however, care must be taken to account for bimolecular processes including triplet−triplet annihilation, singlet−triplet annihilation, and triplet−triplet fusion. Here, we attempt to avoid these issues by applying a device-based methodology capable of specifically probing triplet diffusion at low light fluence in singlet fission materials that is independent of the efficiency of singlet fission or the presence of singlet diffusion. While this method has been previously demonstrated on both emissive and dark organic semiconductors, it has not been applied to systems where there are potentially multiple diffusing species.[20,21] Several archetypical singlet fission materials are considered including pentacene, with a near unity yield of singlet fission,[22] and tetracene and 5,12-bis((triisopropylsilyl)ethynyl)tetracene (TIPS-tetracene), both of which are characterized by singlet and triplet populations in equilibrium.[23] To directly probe triplet exciton diffusion, a triplet injection layer is used to

Received: September 15, 2020
Accepted: January 5, 2021
Published: January 19, 2021

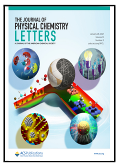

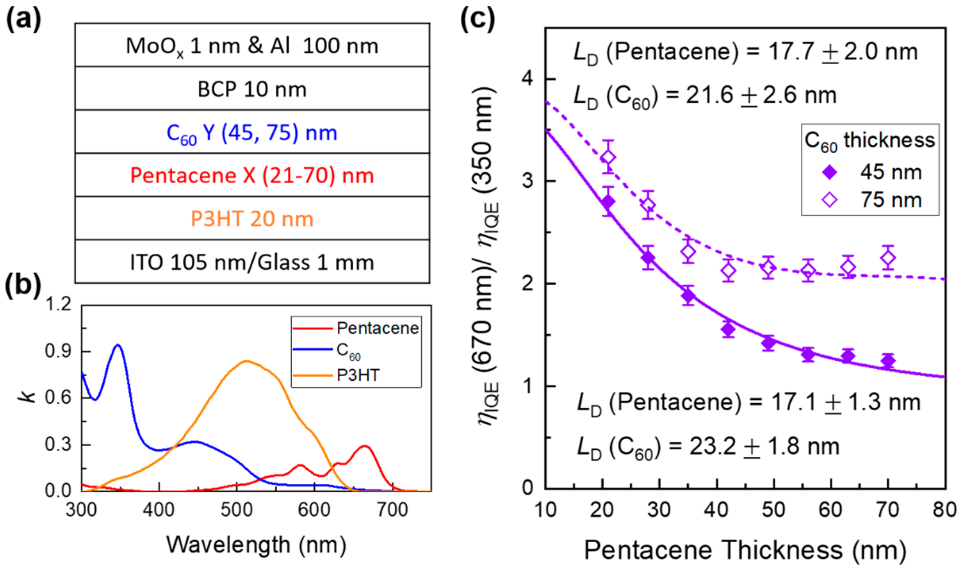

Figure 1. (a) Device architecture for the measurement of L_D in pentacene. (b) Thin film extinction coefficients (k) of pentacene, C$_{60}$, and P3HT. (c) Internal quantum efficiency ratio as a function of pentacene layer thickness for two different C$_{60}$ thicknesses with corresponding values of L_D extracted from fitting.

selectively excite the triplet states and isolate triplet transport from other processes.

Tetracene, pentacene, poly(3-hexylthiophene-2,5-diyl) (P3HT), di-[4-(N,N-di-p-tolylamino)phenyl]cyclohexane (TAPC), platinum phthalocyanine (PtPc), lead phthalocyanine (PbPc), and 1,4,5,8,9,11-hexaazatriphenylene hexacarbonitrile (HATCN) were purchased from Luminescence Technology Corporation. TIPS-tetracene was supplied by Dr. Simon Dowland and Dr. Akshay Rao at the University of Cambridge. C$_{60}$ (99%) was purchased from MER Corporation; MoO$_3$ (99%) and 2,9-dimethyl-4,7-diphenyl-1,10-phenanthroline (BCP) (98%) were obtained from Alfa Aesar. For thickness-dependent photoluminescence (PL) quenching measurements, a unity quenching efficiency is assumed for HATCN due to the favorable energy offset for electron transfer from the donor material.[20,24] Photoluminescence spectra were collected by using a Photon Technology International QuantaMaster 400 fluorometer equipped with a photomultiplier detection system. Thin film samples are pumped by using a monochromated Xe arc lamp at an angle of 70° from substrate normal under N$_2$ purge. The device external quantum efficiency was calculated from the short-circuit current under monochromatic light illumination by using a 300 W Oriel Xe lamp, a monochromator, an optical chopper wheel, and an SR-810 lock-in amplifier. The light intensity at wavelengths of interest was $<10\ \mu$W/cm^2, leading to exciton populations of $\sim 10^{10}$/cm^3, below the onset for triplet−triplet annihilation.[25] Film thicknesses as well as reflectance and transmittance spectra were measured by using a J. A. Woollam variable-angle spectroscopic ellipsometer. Reflectance spectra were measured at an angle of 15° to the substrate normal. Material optical constants were obtained from fitting transmittance (normal incidence) and reflectance spectra. The device internal quantum efficiency was calculated by dividing the measured external quantum efficiency by the absorption efficiency. The absorption efficiency was rigorously calculated by using an optical transfer matrix formalism.[26] Organic photovoltaic cells (OPVs) were fabricated on indium tin oxide (ITO)-coated glass substrates. Substrates were sequentially cleaned in Tergitol solution, deionized water, acetone, and isopropanol, followed by exposure to ambient UV-ozone. Thin film layers were deposited at room temperature by using high-vacuum thermal evaporation at a deposition pressure of $<9 \times 10^{-7}$ Torr. Donor films of pentacene, tetracene, and TIPS-tetracene were deposited at 0.2 nm/s.

The singlet fission process in organic semiconductor materials can be classified as exothermic or endothermic based on the energetic alignment between the singlet energy and twice the triplet energy. The process is exothermic for materials such as pentacene, where the singlet energy exceeds that of the triplet pair ($E(S_1) > 2E(T_1)$).[27] This leads to the rapid and complete conversion of the singlet state, meaning only the triplet will contribute to photocurrent in an OPV when paired with an acceptor such as C$_{60}$.[28] For endothermic materials such as tetracene,[27] the conversion is incomplete, and thus both states may contribute to photocurrent.[29]

In an exothermic fission material like pentacene, triplets are the only diffusing species contributing to photocurrent in and OPV. As such, the triplet L_D can be extracted by using a previously described device-based photocurrent-ratio methodology.[20,21] While prior work has demonstrated the ability to extract L_D by fitting OPV external quantum efficiency (η_{EQE}) spectra,[26] this analysis often yields an underestimate due to interfacial charge transfer (CT) state recombination prior to charge collection.[30,31] The photocurrent-ratio methodology overcomes this limitation by instead fitting a ratio of donor-to-acceptor internal quantum efficiency (η_{IQE}). The ratio cancels out the unknown efficiency of CT state separation (η_{CS}) since these losses are independent of where the exciton is initially generated.[31,32] The free carrier collection efficiency is assumed to be unity at short circuit, consistent with previous work.[30,34,35] The internal quantum efficiency (η_{IQE}) ratio between the donor (D) and acceptor (A) is thus expressed as

$$\frac{\eta_{IQE}^{D}}{\eta_{IQE}^{A}} = \frac{\eta_T \eta_D^{D} \eta_{CS}}{\eta_D^{A} \eta_{CS}} = \frac{\eta_D^{D}}{\eta_D^{A}/\eta_T} \tag{1}$$

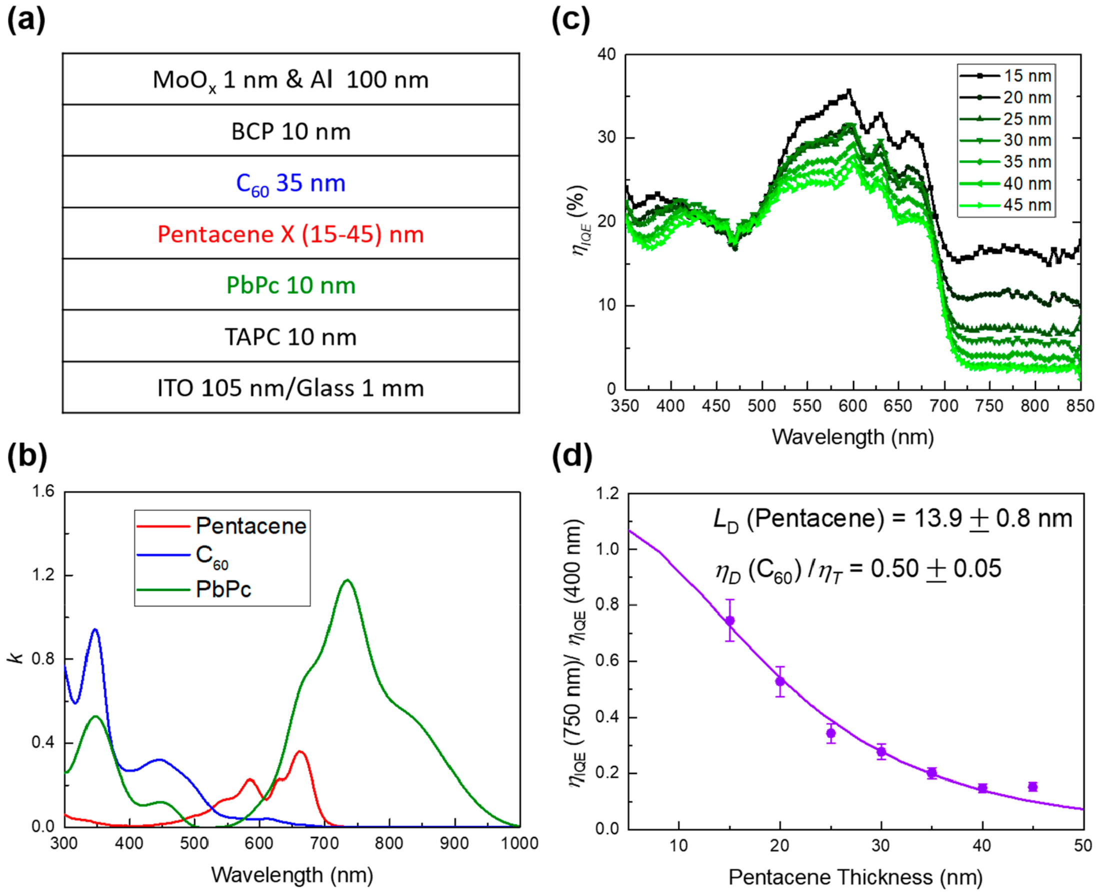

Figure 2. (a) Device architecture for direct injection measurement of pentacene triplet L_D. (b) Extinction coefficients (k) of pentacene, C_{60}, and PbPc. (c) η_{IQE} spectra calculated as the ratio between η_{EQE} and η_A spectra (Figure S2) as a function of pentacene layer thickness. (d) Internal quantum efficiency ratio (λ = 750 nm to λ = 400 nm) as a function of pentacene layer thickness.

where η_T is the triplet yield and here represents the overall efficiency of converting singlets into mobile triplets via fission. The donor diffusion efficiency (η_D^D) will vary with donor thickness while the acceptor diffusion efficiency (η_D^A) will be constant. Because η_T is not expected to vary with donor layer film thickness, it is grouped with η_D^A to create a single thickness-independent fit parameter. Thus, the shape of η_{IQE} ratio as a function of donor thickness is determined by donor η_D^D (numerator) and L_D. Thus, the η_{IQE} ratio is fit to yield the donor L_D and the ratio η_D^A/η_T. If η_T is known, the acceptor L_D may also be determined.

Figure 1a shows the device architecture used to probe the triplet L_D of pentacene. The extinction coefficients of pentacene, C_{60}, and the exciton blocking layer P3HT are shown in Figure 1b. Singlets generated in P3HT may also contribute to photocurrent by Förster transfer to pentacene singlets.[36] To isolate the photoresponse of pentacene and C_{60}, wavelengths of λ = 670 nm (pentacene absorption peak, negligible P3HT absorption) and λ = 350 nm (C_{60} absorption peak, minimal P3HT absorption) are selected for the purposes of comparing donor and acceptor η_{IQE}, respectively (Figure S1). In Figure 1c, the η_{IQE} ratio is fit for two sets of devices having different acceptor thicknesses. Fixing η_T = 200%, the set with a 45 nm thick layer of C_{60} yields a $L_D = 17.1 \pm 1.3$ nm for pentacene and $L_D = 23.2 \pm 1.8$ nm for C_{60}. Devices with a 75 nm thick layer of C_{60} yield similar values, $L_D = 17.7 \pm 2.0$ nm for pentacene and $L_D = 21.6 \pm 2.6$ nm for C_{60}. The value extracted for C_{60} is consistent with the previously reported range of L_D (18–22 nm) extracted by using the same methodology and different donor materials.[20,21] In this configuration of the measurement, knowledge of η_T is required to extract the acceptor L_D and to rule out a contribution from pentacene singlets to the photocurrent.

The photocurrent ratio methodology can be modified to extract the triplet L_D, even when the fission efficiency is not known *a priori* by selectively injecting triplets into the fission material. For example, a triplet injection layer of PbPc (T_1 = 1.02 eV)[37] can be used to selectively inject triplets into pentacene (T_1 = 0.86 eV)[38] via Dexter transfer, circumventing altogether the generation, diffusion, and fission of singlets. The device architecture for this measurement is shown in Figure 2a. In considering eq 1, the ratio is no longer between donor and acceptor but instead between the injector (I) and the acceptor (A) as

$$\frac{\eta_{IQE}^{I}}{\eta_{IQE}^{A}} = \frac{\eta_T \eta_D^I \eta_{CS}}{\eta_D^A \eta_{CS}} = \frac{\eta_D^I}{\eta_D^A/\eta_T} \tag{2}$$

The triplet yield η_T now has a different interpretation, reflecting the efficiency with which triplets are formed in the injector and transferred into pentacene. As triplet energy transfer is typically short-range, triplet exciton generation in pentacene is assumed to occur only in the first monolayer. Again, varying only the donor thickness allows the donor triplet L_D and the ratio η_D^A/η_T to be extracted simultaneously. Figure 2b shows the extinction coefficients of pentacene, C_{60},

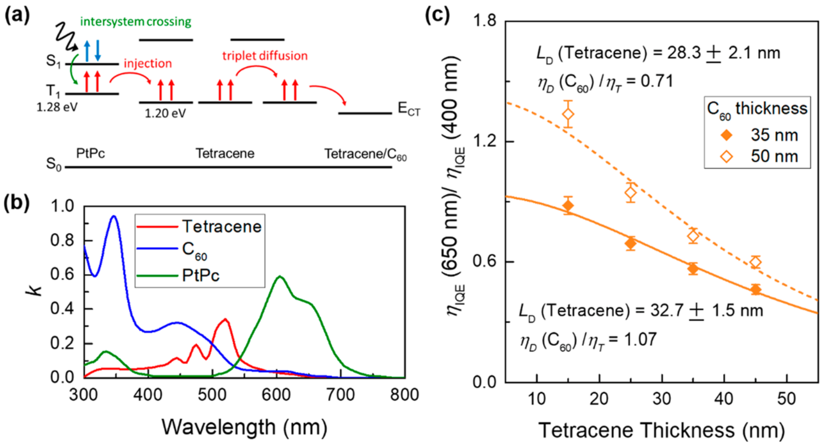

Figure 3. (a) Schematic of energy levels for direct injection measurement of tetracene triplet L_D. (b) Thin film extinction coefficients (k) of tetracene, C_{60}, and PtPc. (c) Internal quantum efficiency ratio (λ = 650 nm to λ = 400 nm) as a function of tetracene layer thickness and C_{60} thickness (solid symbols: 35 nm C_{60} layer; open symbols: 50 nm C_{60} layer). Tetracene triplet L_D values and $\eta_D(C_{60})/\eta_T$ are extracted by fitting each set of data.

and PbPc. The injection layer η_{IQE} is extracted at λ = 750 nm while the acceptor η_{IQE} is extracted at λ = 400 nm (Figure 2c and Figure S2). Fitting the resultant PbPc-C_{60} η_{IQE} ratio as a function of donor thickness (Figure 2d) yields $\eta_D^A/\eta_T = 0.5 \pm 0.05$ and a pentacene triplet L_D = 13.9 ± 0.8 nm, similar to the result 17.1 ± 2.0 nm in Figure 1. The small difference in extracted L_D may reflect the presence of a mobile triplet pair, singlet diffusion, or slight variations in pentacene film morphology. This further reinforces the value of the injector method to selectively and directly interrogate the triplet.

The use of a triplet injection layer also permits probing of triplets in endothermic fission materials such as tetracene where both singlet and triplet diffusion may be relevant under optical excitation. Here, a triplet injection layer of PtPc is used to selectively excite the triplet state of tetracene (Figure 3a). Figure 3b shows the extinction coefficients of tetracene, C_{60}, and PtPc. The injection layer η_{IQE} is extracted at λ = 650 nm (in the absence of absorption from tetracene and C_{60}) while the acceptor η_{IQE} is extracted at λ = 400 nm. Figure 3c shows the PtPc-C_{60} η_{IQE} ratio as a function of tetracene thickness obtained from OPVs with a structure: ITO/10 nm TAPC/10 nm PtPc/X (= 15−45) nm tetracene/Y (= 35, 50) nm C_{60}/10 nm BCP/1 nm MoO_x/100 nm Al. The dependence of the triplet injector−acceptor η_{IQE} ratio on tetracene thickness is fit for devices with a 35 nm thick layer of C_{60}, yielding a triplet L_D = 32.7 ± 1.5 nm for tetracene and $\eta_D(C_{60})/\eta_T$ = 1.07. Devices with a 50 nm thick layer of C_{60} yield a triplet L_D of 28.3 ± 2.1 nm for tetracene and $\eta_D(C_{60})/\eta_T$ = 0.71. The variation in $\eta_D(C_{60})/\eta_T$ with thickness likely reflects reduced exciton harvesting in a thicker acceptor layer of C_{60}. Assuming the C_{60} L_D is the same for both sets of devices, simultaneous fitting yields a triplet L_D of 32.1 ± 2.6 nm for tetracene, L_D = 25.7 ± 1.9 nm for C_{60}, and η_T = 57%. For comparison, thickness-dependent photoluminescence quenching was used to measure the singlet L_D in tetracene (Figure S5) to be 4.0 ± 1.2 nm.

The same method is also applied to TIPS-tetracene, having the same molecular core as tetracene but made compatible with solution processing via addition of triisopropylsilyl (TIPS) side groups. Singlet fission in TIPS-tetracene has been extensively studied both in the solid state and in solution.[39−42] It is endothermic by about 200 meV, and the triplet pair separation time is highly sensitive to morphology.[41] The functionalization of the tetracene core also changes the ionization potential for charge carriers in thin films by 0.38 eV.[43] Therefore, with TIPS-tetracene, C_{60} cannot be used as an acceptor since the lower-energy, interfacial CT state (~1.5 eV as estimated from molecular orbital energy levels)[44] exceeds the TIPS-tetracene triplet energy (1.25 eV).[41] An acceptor layer of HATCN is selected to dissociate the TIPS-tetracene triplet due to its lower lying lowest unoccupied molecular orbital energy level.[45,46] Figure 4a shows the extinction coefficients of TIPS-tetracene, HATCN, and PtPc. The following OPV architecture was used to probe the triplet L_D of TIPS-tetracene: ITO/5 nm PtPc/X (= 6−21) nm TIPS-tetracene/32 nm HATCN/100 nm Al. The measured η_{EQE} spectra are shown in Figure 4b. The injection layer η_{IQE} is extracted at λ = 650 nm (in the absence of absorption from TIPS-tetracene and HATCN) while the acceptor η_{IQE} is extracted at λ = 345 nm. Fitting the resulting η_{IQE} ratio as a function of TIPS-tetracene thickness (Figure 4c) yields a TIPS-tetracene triplet L_D of 3.3 ± 0.4 nm and η_D(HATCN)/η_T = 0.37. As with tetracene, thickness-dependent photoluminescence quenching was used to measure the singlet L_D in TIPS-tetracene (Figure S6) to be significantly longer at 7.1 ± 1.4 nm. We note that devices based on solution-processed (spin coated from solutions of TIPS-Tc in toluene at 5000 rpm) layers of TIPS-tetracene were also measured but showed low reproducibility and a potential variation in film morphology with thickness.

In considering the origin of the wide range in measured triplet L_D values, it is helpful to first isolate differences in triplet exciton lifetime. Prior reports suggest a range of 40−200 ns for polycrystalline tetracene films,[25] 5 ns for polycrystalline pentacene films,[47] and 570 ns for disordered TIPS-tetracene films.[25] Clearly, the observed trend in triplet L_D of 32.1 ± 2.6 nm for tetracene, 17.1 ± 1.3 nm for pentacene, and 3.3 ± 0.4 nm for TIPS-tetracene does not reflect a simple dependence on exciton lifetime. We hypothesize that the observed trend reflects changes in the triplet exciton diffusivity arising from differences in crystalline grain size or intermolecular spacing and packing.[48,49] A more detailed study is required to fully explore the factors leading to differences in triplet L_D.

We present a device-based, photocurrent-ratio approach capable of extracting the triplet diffusion length in singlet

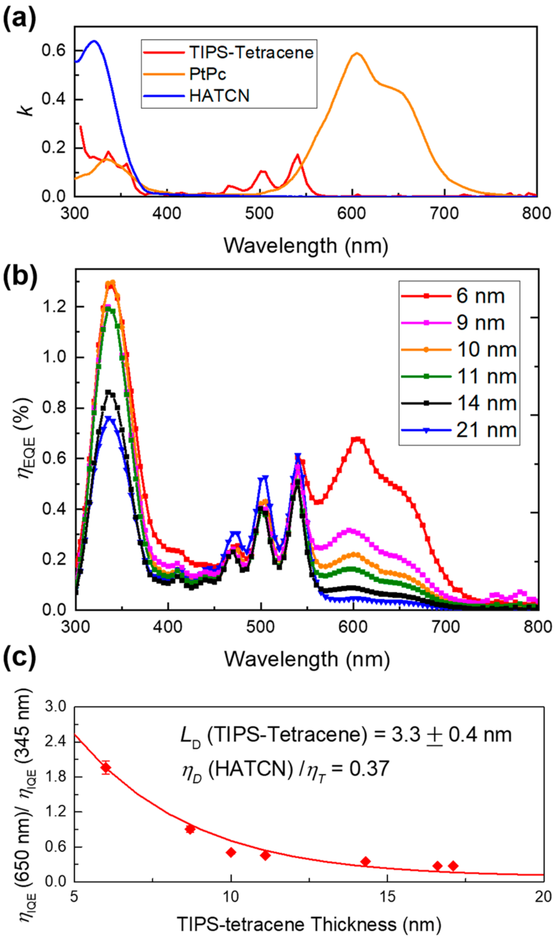

Figure 4. (a) Extinction coefficient (k) of device active layers. (b) η_{EQE} spectra measured as a function of TIPS-tetracene layer thickness. (c) η_{IQE} ratio as a function of TIPS-tetracene layer thickness. TIPS-tetracene triplet L_D values and $\eta_D(\text{HATCN})/\eta_T$ are extracted by fitting η_{IQE} ratio as a function of thickness.

fission materials. This method allows measurement of the triplet L_D in isolation from carrier recombination, singlet diffusion, triplet fusion, and singlet fission, removing several common sources of uncertainty. This is enabled by the use of a triplet injector layer that isolates excitation to the triplet state of the material of interest. Indeed, we can extract the triplet L_D even when the singlet fission efficiency is not known *a priori*. The triplet L_D is extracted for several archetypical materials, yielding values of 32.1 ± 2.6 nm for tetracene, 17.1 ± 1.3 nm for pentacene, and 3.3 ± 0.4 nm for TIPS-tetracene. The ability to directly interrogate triplet diffusion in OPVs offers new opportunities for the study of intrinsic structure−property relationships to better enable the use of triplet excitons in photoconversion.

■ ASSOCIATED CONTENT

Supporting Information

The Supporting Information is available free of charge at https://pubs.acs.org/doi/10.1021/acs.jpclett.0c02825.

Additional device data used to analyze triplet exciton transport and photoluminescence quenching results used to extract singlet exciton diffusion lengths for tetracene and TIPS-tetracene (PDF)

■ AUTHOR INFORMATION

Corresponding Author

Russell J. Holmes − *Department of Chemical Engineering and Materials Science, University of Minnesota, Minneapolis, Minnesota 55455, United States*; orcid.org/0000-0001-7183-3673; Email: rholmes@umn.edu

Authors

Tao Zhang − *Department of Chemical Engineering and Materials Science, University of Minnesota, Minneapolis, Minnesota 55455, United States*; orcid.org/0000-0002-6582-1892

Deepesh Rai − *Department of Chemical Engineering and Materials Science, University of Minnesota, Minneapolis, Minnesota 55455, United States*

Complete contact information is available at: https://pubs.acs.org/10.1021/acs.jpclett.0c02825

Author Contributions

T.Z. and D.R. equally contributed to this work.

Notes

The authors declare no competing financial interest.

■ ACKNOWLEDGMENTS

This work was supported by National Science Foundation (NSF) Electronics, Photonics and Magnetic Devices under ECCS-1509121 and Solid-State and Materials Chemistry under DMR-1708177. T.Z. acknowledges support from a University of Minnesota Doctoral Dissertation Fellowship. R.J.H. acknowledges support from Ronald L. and Janet A. Christenson, a Leverhulme Trust Visiting Professorship at the University of Cambridge, and a Visiting Fellowship at Clare Hall, University of Cambridge. R.J.H. also thanks Dr. Simon Dowland, Dr. Aksahy Rao, and Prof. Richard Friend for useful discussions.

■ REFERENCES

(1) Xia, J.; Sanders, S. N.; Cheng, W.; Low, J. Z.; Liu, J.; Campos, L. M.; Sun, T. Singlet Fission: Progress and Prospects in Solar Cells. *Adv. Mater.* **2017**, *29*, 1601652.

(2) Miyata, K.; Conrad-Burton, F. S.; Geyer, F. L.; Zhu, X.-Y. Triplet Pair States in Singlet Fission. *Chem. Rev.* **2019**, *119*, 4261−4292.

(3) Rao, A.; Friend, R. H. Harnessing Singlet Exciton Fission to Break the Shockley−Queisser Limit. *Nat. Rev. Mater.* **2017**, *2*, 17063.

(4) Basel, B. S.; Papadopoulos, I.; Thiel, D.; Casillas, R.; Zirzlmeier, J.; Clark, T.; Guldi, D. M.; Tykwinski, R. R. Pentacenes: A Molecular Ruler for Singlet Fission. *Trends Chem.* **2019**, *1*, 11−21.

(5) Felter, K. M.; Grozema, F. C. Singlet Fission in Crystalline Organic Materials: Recent Insights and Future Directions. *J. Phys. Chem. Lett.* **2019**, *10*, 7208−7214.

(6) Piland, G. B.; Burdett, J. J.; Dillon, R. J.; Bardeen, C. J. Singlet Fission: From Coherences to Kinetics. *J. Phys. Chem. Lett.* **2014**, *5*, 2312−2319.

(7) Einzinger, M.; Wu, T.; Kompalla, J. F.; Smith, H. L.; Perkinson, C. F.; Nienhaus, L.; Wieghold, S.; Congreve, D. N.; Kahn, A.; Bawendi, M. G.; et al. Sensitization of Silicon by Singlet Exciton Fission in Tetracene. *Nature* **2019**, *571*, 90−94.

(8) Futscher, M. H.; Rao, A.; Ehrler, B. The Potential of Singlet Fission Photon Multipliers as an Alternative to Silicon-Based Tandem Solar Cells. *ACS Energy Lett.* **2018**, *3*, 2587−2592.

(9) MacQueen, R. W.; Liebhaber, M.; Niederhausen, J.; Mews, M.; Gersmann, C.; Jäckle, S.; Jäger, K.; Tayebjee, M. J. Y.; Schmidt, T. W.; Rech, B.; et al. Crystalline Silicon Solar Cells with Tetracene Interlayers: The Path to Silicon-Singlet Fission Heterojunction Devices. *Mater. Horiz.* **2018**, *5*, 1065−1075.

(10) Pazos-Outón, L. M.; Lee, J. M.; Futscher, M. H.; Kirch, A.; Tabachnyk, M.; Friend, R. H.; Ehrler, B. A Silicon−Singlet Fission Tandem Solar Cell Exceeding 100% External Quantum Efficiency with High Spectral Stability. *ACS Energy Lett.* **2017**, *2*, 476−480.

(11) Burdett, J. J.; Gosztola, D.; Bardeen, C. J. The Dependence of Singlet Exciton Relaxation on Excitation Density and Temperature in Polycrystalline Tetracene Thin Films: Kinetic Evidence for a Dark Intermediate State and Implications for Singlet Fission. *J. Chem. Phys.* **2011**, *135*, 214508.

(12) Chan, W.-L.; Ligges, M.; Jailaubekov, A.; Kaake, L.; Miaja-Avila, L.; Zhu, X. Y. Observing the Multiexciton State in Singlet Fission and Ensuing Ultrafast Multielectron Transfer. *Science (Washington, DC, U. S.)* **2011**, *334*, 1541−1545.

(13) Zimmerman, P. M.; Zhang, Z.; Musgrave, C. B. Singlet Fission in Pentacene through Multi-Exciton Quantum States. *Nat. Chem.* **2010**, *2*, 648−652.

(14) Akselrod, G. M.; Deotare, P. B.; Thompson, N. J.; Lee, J.; Tisdale, W. A.; Baldo, M. A.; Menon, V. M.; Bulović, V.; Bulovic, V.; Bulović, V. Visualization of Exciton Transport in Ordered and Disordered Molecular Solids. *Nat. Commun.* **2014**, *5*, 3646.

(15) Tayebjee, M. J. Y.; Clady, R. G. C. R.; Schmidt, T. W. The Exciton Dynamics in Tetracene Thin Films. *Phys. Chem. Chem. Phys.* **2013**, *15*, 14797−14805.

(16) Zhu, T.; Huang, L. Exciton Transport in Singlet Fission Materials: A New Hare and Tortoise Story. *J. Phys. Chem. Lett.* **2018**, *9*, 6502−6510.

(17) Zhu, T.; Wan, Y.; Guo, Z.; Johnson, J.; Huang, L. Two Birds with One Stone: Tailoring Singlet Fission for Both Triplet Yield and Exciton Diffusion Length. *Adv. Mater.* **2016**, *28*, 7539−7547.

(18) Wan, Y.; Guo, Z.; Zhu, T.; Yan, S.; Johnson, J.; Huang, L. Cooperative Singlet and Triplet Exciton Transport in Tetracene Crystals Visualized by Ultrafast Microscopy. *Nat. Chem.* **2015**, *7*, 785−792.

(19) Grieco, C.; Doucette, G. S.; Pensack, R. D.; Payne, M. M.; Rimshaw, A.; Scholes, G. D.; Anthony, J. E.; Asbury, J. B. Dynamic Exchange During Triplet Transport in Nanocrystalline TIPS-Pentacene Films. *J. Am. Chem. Soc.* **2016**, *138*, 16069−16080.

(20) Zhang, T.; Dement, D. B.; Ferry, V. E.; Holmes, R. J. Intrinsic Measurements of Exciton Transport in Photovoltaic Cells. *Nat. Commun.* **2019**, *10*, 1156.

(21) Shi, K.; Curtin, I. J.; Healy, A. T.; Zhang, T.; Rai, D.; Blank, D. A.; Holmes, R. J. Probing Enhanced Exciton Diffusion in a Triplet-Sensitized Organic Photovoltaic Cell. *J. Phys. Chem. C* **2020**, *124*, 3489−3495.

(22) Congreve, D. N.; Lee, J.; Thompson, N. J.; Hontz, E.; Yost, S. R.; Reusswig, P. D.; Bahlke, M. E.; Reineke, S.; Van Voorhis, T.; Baldo, M. A. External Quantum Efficiency Above 100% in a Singlet-Exciton-Fission-Based Organic Photovoltaic Cell. *Science (Washington, DC, U. S.)* **2013**, *340*, 334−337.

(23) Jadhav, P. J.; Mohanty, A.; Sussman, J.; Lee, J.; Baldo, M. A. Singlet Exciton Fission in Nanostructured Organic Solar Cells. *Nano Lett.* **2011**, *11*, 1495−1498.

(24) Menke, S. M.; Holmes, R. J. Energy-Cascade Organic Photovoltaic Devices Incorporating a Host−Guest Architecture. *ACS Appl. Mater. Interfaces* **2015**, *7*, 2912−2918.

(25) Burdett, J. J.; Müller, A. M.; Gosztola, D.; Bardeen, C. J. Excited State Dynamics in Solid and Monomeric Tetracene: The Roles of Superradiance and Exciton Fission. *J. Chem. Phys.* **2010**, *133*, 144506.

(26) Pettersson, L. A. A.; Roman, L. S.; Inganäs, O. Modeling Photocurrent Action Spectra of Photovoltaic Devices Based on Organic Thin Films. *J. Appl. Phys.* **1999**, *86*, 487−496.

(27) Zimmerman, P. M.; Bell, F.; Casanova, D.; Head-Gordon, M. Mechanism for Singlet Fission in Pentacene and Tetracene: From Single Exciton to Two Triplets. *J. Am. Chem. Soc.* **2011**, *133*, 19944−19952.

(28) Zhang, Y. J.; Li, P.; Cai, L.; Xiang, J.; Ding, B. F.; Alameh, K.; Song, Q. L. A Simple and Cost Effective Experimental Method for Verifying Singlet Fission in Pentacene−C_{60} Solar Cells. *RSC Adv.* **2015**, *5*, 29718−29722.

(29) Wu, T. C.; Thompson, N. J.; Congreve, D. N.; Hontz, E.; Yost, S. R.; Van Voorhis, T.; Baldo, M. A. Singlet Fission Efficiency in Tetracene-Based Organic Solar Cells. *Appl. Phys. Lett.* **2014**, *104*, 193901.

(30) Mullenbach, T. K.; Curtin, I. J.; Zhang, T.; Holmes, R. J. Probing Dark Exciton Diffusion Using Photovoltage. *Nat. Commun.* **2017**, *8*, 14215.

(31) Curtin, I. J.; Holmes, R. J. Decoupling Photocurrent Loss Mechanisms in Photovoltaic Cells Using Complementary Measurements of Exciton Diffusion. *Adv. Energy Mater.* **2018**, *8*, 1702339.

(32) Kurpiers, J.; Ferron, T.; Roland, S.; Jakoby, M.; Thiede, T.; Jaiser, F.; Albrecht, S.; Janietz, S.; Collins, B. A.; Howard, I. A.; Neher, D. Probing the Pathways of Free Charge Generation in Organic Bulk Heterojunction Solar Cells. *Nat. Commun.* **2018**, *9*, 2038.

(33) Vandewal, K.; Albrecht, S.; Hoke, E. T.; Graham, K. R.; Widmer, J.; Douglas, J. D.; Schubert, M.; Mateker, W. R.; Bloking, J. T.; Burkhard, G. F.; et al. Efficient Charge Generation by Relaxed Charge-Transfer States at Organic Interfaces. *Nat. Mater.* **2014**, *13*, 63−68.

(34) Zhang, T.; Holmes, R. J. Photovoltage as a Quantitative Probe of Carrier Generation and Recombination in Organic Photovoltaic Cells. *J. Mater. Chem. C* **2017**, *5*, 11885−11891.

(35) Nakano, K.; Chen, Y.; Xiao, B.; Han, W.; Huang, J.; Yoshida, H.; Zhou, E.; Tajima, K. Anatomy of the Energetic Driving Force for Charge Generation in Organic Solar Cells. *Nat. Commun.* **2019**, *10*, 2520.

(36) Tabachnyk, M.; Ehrler, B.; Bayliss, S.; Friend, R. H.; Greenham, N. C. Triplet Diffusion in Singlet Exciton Fission Sensitized Pentacene Solar Cells. *Appl. Phys. Lett.* **2013**, *103*, 153302.

(37) Minami, N. Photocurrent Spectra of Phthalocyanine Thin-Film Electrodes in the Visible to near-Infrared. *J. Chem. Soc., Faraday Trans. 2* **1982**, *78*, 1871−1880.

(38) Ehrler, B.; Walker, B. J.; Böhm, M. L.; Wilson, M. W. B.; Vaynzof, Y.; Friend, R. H.; Greenham, N. C. In Situ Measurement of Exciton Energy in Hybrid Singlet-Fission Solar Cells. *Nat. Commun.* **2012**, *3*, 1019.

(39) Pace, N. A.; Arias, D. H.; Granger, D. B.; Christensen, S.; Anthony, J. E.; Johnson, J. C. Dynamics of Singlet Fission and Electron Injection in Self-Assembled Acene Monolayers on Titanium Dioxide. *Chem. Sci.* **2018**, *9*, 3004−3013.

(40) Stern, H. L.; Musser, A. J.; Gelinas, S.; Parkinson, P.; Herz, L. M.; Bruzek, M. J.; Anthony, J.; Friend, R. H.; Walker, B. J. Identification of a Triplet Pair Intermediate in Singlet Exciton Fission in Solution. *Proc. Natl. Acad. Sci. U. S. A.* **2015**, *112*, 7656−7661.

(41) Stern, H. L.; Cheminal, A.; Yost, S. R.; Broch, K.; Bayliss, S. L.; Chen, K.; Tabachnyk, M.; Thorley, K.; Greenham, N.; Hodgkiss, J. M.; et al. Vibronically Coherent Ultrafast Triplet-Pair Formation and Subsequent Thermally Activated Dissociation Control Efficient Endothermic Singlet Fission. *Nat. Chem.* **2017**, *9*, 1205−1212.

(42) Dover, C. B.; Gallaher, J. K.; Frazer, L.; Tapping, P. C.; Petty, A. J.; Crossley, M. J.; Anthony, J. E.; Kee, T. W.; Schmidt, T. W. Endothermic Singlet Fission Is Hindered by Excimer Formation. *Nat. Chem.* **2018**, *10*, 305−310.

(43) Griffith, O. L.; Jones, A. G.; Anthony, J. E.; Lichtenberger, D. L. Intermolecular Effects on the Hole States of Triisopropylsilylethynyl-Substituted Oligoacenes. *J. Phys. Chem. C* **2010**, *114*, 13838−13845.

(44) Ohno, T. R.; Chen, Y.; Harvey, S. E.; Kroll, G. H.; Weaver, J. H.; Haufler, R. E.; Smalley, R. E. Bonding and Energy-Level Alignment on Metal and Semiconductor Surfaces. *Phys. Rev. B: Condens. Matter Mater. Phys.* **1991**, *44*, 13747−13755.

(45) Oh, E.; Park, S.; Jeong, J.; Kang, S. J.; Lee, H.; Yi, Y. Energy Level Alignment at the Interface of NPB/HAT-CN/Graphene for Flexible Organic Light-Emitting Diodes. *Chem. Phys. Lett.* **2017**, *668*, 64−68.

(46) Wang, H.; He, Y.; Li, Y.; Su, H. Photophysical and Electronic Properties of Five PCBM-like C_{60} Derivatives: Spectral and Quantum Chemical View. *J. Phys. Chem. A* **2012**, *116*, 255−262.

(47) Rao, A.; Wilson, M. W. B.; Hodgkiss, J. M.; Albert-Seifried, S.; Bässler, H.; Friend, R. H. Exciton Fission and Charge Generation via

Triplet Excitons in Pentacene/C_{60} Bilayers. *J. Am. Chem. Soc.* **2010**, *132*, 12698−12703.

(48) Rai, D.; Bangsund, J. S.; Barriocanal, J. G.; Holmes, R. J. Impact of Molecular Structure on Singlet and Triplet Exciton Diffusion in Phenanthroline Derivatives. *J. Mater. Chem. C* **2020**, *8*, 6118−6123.

(49) Lunt, R. R.; Benziger, J. B.; Forrest, S. R. Relationship between Crystalline Order and Exciton Diffusion Length in Molecular Organic Semiconductors. *Adv. Mater.* **2010**, *22*, 1233−1236.